Journal of Pharmacopuncture

ISSN 2093-6966 [Print], ISSN 2234-6856 [Online]
Journal of Pharmacopuncture 2016;19[1]:037-044
DOI: http://dx.doi.org/10.3831/KPI.2016.19.005

Original article

Nanopharmaceutical Approach for Enhanced Anti-cancer Activity of Betulinic Acid in Lung-cancer Treatment via Activation of PARP: Interaction with DNA as a Target

-Anti-cancer Potential of Nano-betulinic Acid in Lung Cancer-

Jayeeta Das[1], Asmita Samadder[1,2], Sreemanti Das[1], Avijit Paul[1], Anisur Rahman Khuda-Bukhsh[1]*

[1] Cytogenetics and Molecular Biology Laboratory, Department of Zoology, University of Kalyani, Kalyani, India
[2] Department of Zoology, Dumdum Motijheel College, Kolkata, India

Key Words

A549 cell line, betulinic acid, drug-DNA interaction, mice, poly (lactide-co-glycolide)

Abstract

Objectives: This study examined the relative efficacies of a derivative of betulinic acid (dBA) and its poly (lactide-co-glycolide) (PLGA) nano-encapsulated form in A549 lung cancer cells *in vivo* and in co-mutagen [sodium arsenite (SA) + benzo[a]pyrene (BaP)]-induced lung cancer in mice *in vivo*.

Methods: dBA was loaded with PLGA nanoparticles by using the standard solvent displacement method. The sizes and morphologies of nano-dBA (NdBA) were determined by using transmission electron microscopy (TEM), and their intracellular localization was verified by using confocal microscopy. The binding and interaction of NdBA with calf thymus deoxyribonucleic acid (CT-DNA) as a target were analyzed by using conventional circular dichroism (CD) and melting temperature (Tm) profile data. Apoptotic signalling cascades *in vitro* and *in vivo* were studied by using an enzyme-linked immunosorbent assay (ELISA); the ability of NdBA to cross the blood-brain barrier (BBB) was also examined. The stage of cell cycle arrest was confirmed by using a fluorescence-activated cell-sorting (FACS) data analysis.

Results: The average size of the nanoparticles was ~ 110 nm. Confocal microscopy images confirmed the presence of NdBA in the cellular cytoplasm. The bio-physical properties of dBA and NdBA ascertained from the CD and the Tm profiles revealed that NdBA had greater interaction with the target DNA than dBA did. Both dBA and NdBA arrested cell proliferation at G0/G1, NdBA showing the greater effect. NdBA also induced a greater degree of cytotoxicity in A549 cells, but it had an insignificant cytotoxic effect in normal L6 cells. The results of flow cytometric, cytogenetial and histopathological studies in mice revealed that NdBA caused less nuclear condensation and DNA damage than dBA did. TEM images showed the presence of NdBA in brain samples of NdBA fed mice, indicating its ability to cross the BBB.

Conclusion: Thus, compared to dBA, NdBA appears to have greater chemoprotective potential against lung cancer.

Received: Dec 30, 2015 **Reviewed:** Jan 25, 2015 **Accepted:** Feb 03, 2016

1. Introduction

Polyaromatic hydrocarbons (PAHs) and arsenic are well-known environmental toxicants. They have detrimental effects on living organisms. Benzo[a]pyrene (BaP) is one member of the PAH family and has been

*Corresponding Author
Anisur Rahman Khuda-Bukhsh. Cytogenetics and Molecular Biology Laboratory, Department of Zoology, University of Kalyani, Kalyani-741235, India.
Tel: +91-33-25828768 Fax: +91-33-25828282
Email: prof_arkb@yahoo.co.in; khudabukhsh_48@rediffmail.com

strongly implicated as a cause of human adenomatous lung tumors [1]. Arsenic, administered with a potent carcinogen like BaP, synergistically enhances the carcinogenic action of BaP. BaP produces deoxyribonucleic acid (DNA)-adduct in the form of benzo[a]pyrene diol epoxide-N2-deoxyguanosine (BPDE-N2-dG), which is considered to be the critical event in carcinogenicity, leading to lung cancer. Cancer cells often resort to a variety of adaptations and responses that make them drug-resistant; they often carry mutations that make the apoptotic machinery ineffective, helping them to evade apoptosis or cell death signals. On the other hand, ideal and effective drugs for therapeutic use should be endowed with properties that are sufficiently strong to give them the ability to overcome the drug-resistance of cancer cells and induce apoptosis. Drugs with such abilities are the ones that are highly solicited for use in oncotherapy.

Most cases of lung cancer are incurable, but proper treatment can prolong life for many and help sustain a good quality of life. Inevitably, disease-related symptoms develop with the progression of the disease, and these may be difficult to differentiate from treatment-induced complications because most orthodox anti-cancer drugs have their own toxic side-effects. Thus, physicians now a days look for some suitable supportive medication from complementary and alternative medicine (CAM) to give lung cancer patients a better quality of life. Complementary therapies are, thus, playing an increasingly important role in the control and management of cancer [2]. The use of biological-based CAM, such as herbs, different phytochemicals, and other dietary supplements, are now becoming popular for treating cancer patients.

Phytolacca decandra (PD), belonging to the *Phytolaccaceae* family, is commonly known as pokeweed. It has been reported to be used in the treatment of tumors, oedema, bronchitis, and abscesses, as stated in ancient literature [3]. Likewise, the extract of a congeneric species, *Phytolacca americana*, has been reported to contain triterpene saponins (phytolacca saponin), phytolaccagenic acid, phytolaccagenin, etc. [4]. Das *et al* [5] also reported that the dried root extract of PD could be effectively encapsulated in poly (lactide-co-glycolide) (PLGA) polymers; these nano-capsules showed greater anti-cancer effect than their un-encapsulated counterparts when tested against lung cancer. However, to our knowledge, studies on the anti-cancer potential of any isolated major bioactive ingredient of PD or its PLGA-loaded nano form have not yet been undertaken. Therefore, we became interested in isolating one of the major ingredients of PD, namely, 1-isopropenyl-5a,5b,8,8,11a-pentamethyl-1,2,3,4,5,5a,6,7,7a,8,11,11a,11b,12,13,13a,13b-octadecahydro cyclopenta[a]chrysene3a-carboxylic acid, a derivative of betulinic acid (dBA), and contemplated examining its anti-cancer potential, if any, through well-established scientific protocols.

In our earlier report [5], we first investigated the effects of both a dBA and a nano-dBA (NdBA) on A549 cancer cells *in vitro* because this cell line has a K-ras mutation that gives its cells the ability to skip most apoptosis-inducing signals, thereby making them drug-resistant against most orthodox therapeutic drugs. However, we were quite fascinated with the results that showed dBA and NdBA induce apoptosis in these cancer cells through a mitochondrial intrinsic pathway. NdBA was found to have greater anti-cancer potential than dBA against A549 cells *in vitro*. Therefore, we became interested in further testing its effects in a mammalian model, mice, which have close genetic semblances with human beings, to explore if it had similar effects in mice and to further evaluate the possibility of its use in humans in future drug development and oncotherapy.

Thus, the major objectives of the present study were i) to test the anticancer potential of dBA, the major active ingredient of PD, if any, ii) to strategically nano-encapsulate dBA by using PLGA polymers to produce NdBA, iii) to characterize NdBA physico-chemically to evaluate the relative efficacies of dBA and NdBA to ascertain if NdBA had enhanced chemo-protective action in lung cancer cells of mice *in vivo* induced by a co-mutagenic treatment of BaP and sodium arsenite (SA), iv) to examine if NdBA could cross the blood-brain barrier (BBB) and v) to evaluate the relative efficacies of dBA and NdBA in inducing apoptosis and highlight the probable signaling cascades and roles of the drug-DNA interactions involved in the process.

2. Materials and Methods

All the chemicals used in this study were procured from Sigma, USA, and were of analytical grade. Following the solvent displacement method of Fessi *et al* [6], PLGA encapsulation of dBA was done under optimal conditions. For blank nanoparticles, the same method was used, but without the addition of dBA during the preparation. An aqueous suspension of NdBA was prepared for transmission electron microscopy (TEM) measurements by placing a drop of the suspension on a copper grid and allowing the water to evaporate. TEM observations were made using a JEOL-2100F electron microscope operated at an accelerating voltage of 200 kV.

Circular dichroic spectral analysis were done by using a Jasco spectropolarimeter (J-720) monitored at 25°C. Changes in the structure of calf thymus DNA (CT-DNA) in the wavelength region of 200 – 650 nm were detected by using a 1-m path-length rectangular quartz cuvette. Melting temperature (Tm) profile data for CT-DNA, CT-DNA + dBA and CT-DNA + NdBA were obtained with the aid of a SHIMADZU-UV-1700 spectrophotometer fitted with a temperature program. CT-DNA is generally used as a target for understanding possible drug - DNA interactions in human DNA. Fragmentation assays of CT-DNA, CT-DNA + dBA and CT-DNA + NdBA were performed by using gel electrophoresis in 1% agarose gel [7].

Human non-small-cell lung carcinoma cells, A549, were procured from NCCS, Pune, India. The cells were cultured at 5×10^5 cells/mL in Dulbecco's Modified Eagle's Medium (DMEM) supplemented with 10% fetal bovine serum and 1% Penicillin-Streptomycin-Neomycin (PSN) antibiotic at 37°C and 5% CO_2 for experimental purposes. The A549 lung cancer cells were cultured at 10^5 cells/mL confluence. Cells were treated with different concentrations of dBA and NdBA, and the anti-proliferative effects were determined

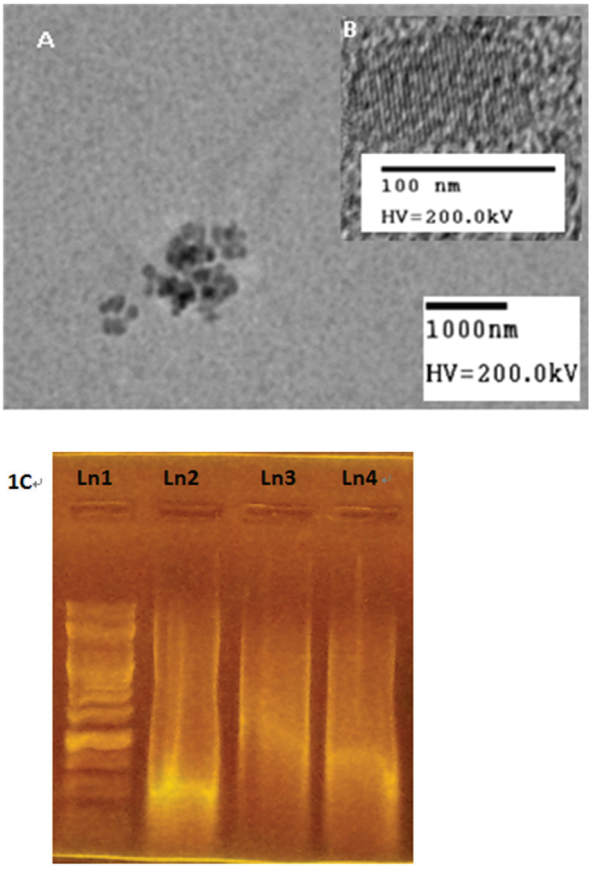

Figure 1 TEM images of (A) at low magnification (12000X) and (B) at high magnification (HRTEM, 800000X). (C) CT-DNA fragmentation assay: Ln1 = DNA ladder, Ln2 = CT-DNA, Ln3 = CT-DNA + dBA, and Ln4 = CT-DNA + NdBA.

TEM, transmission electron microscopy; CT-DNA, calf thymus deoxyribonucleic acid; NdBA, nano derivative of betulinic acid.

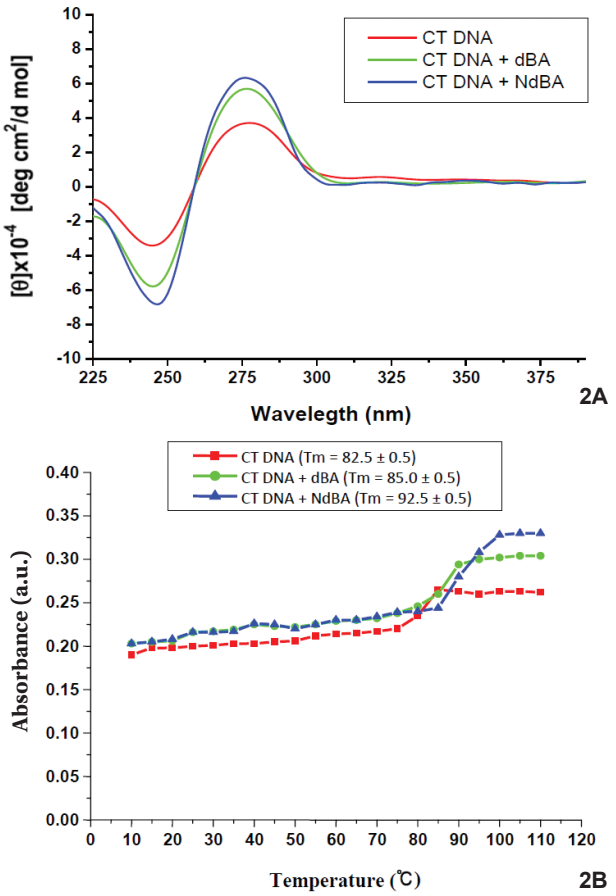

Figure 2 (A) CD pectral analyses and (B) Tm profiles of CT-DNA alone, CT-DNA + dBA and CT-DNA + NdBA.

CT DNA, calf thymus deoxyribonucleic acid; dBA, derivative of betulinic acid; NdBA, nano derivative of betulinic acid; Tm, melting temperature; CD, circular dichroic.

using trypan blue [7]. PLGA blank nanoparticles served as controls. Similar experiments were also performed in L6 skeletal muscle cells to check the cytotoxic effect, if any, of dBA and NdBA in normal cells. To test whether NdBA was localized in the cell's cytoplasm or it had entered the nucleus, we exposed A549 cells to 50 μg/mL of fluorescein isothiocyanate (FITC)-PLGA and/or FITC-PLGA-dBA. Cells were then washed with phosphate buffer solution (PBS), fixed in 70% ethanol for 1 hour at room temperature and studied under confocal microscope [8].

Expressions of poly [adenosine diphosphate (ADP)-ribose] polymerase (PARP), Bcl2 Antagonist X (Bax) and B-cell lymphoma 2 (Bcl2) proteins were analyzed by using anti-PARP, anti-caspase 3, anti-Bax and anti-Bcl2 primary antibodies (Santa Cruz Biotechnology, Inc., USA) and alkaline- phosphatase-conjugated secondary antibodies (Sigma Aldrich, USA) following the standard technique for the indirect enzyme-linked immunosorbent assay (ELISA) [7]. The absorbance was measured at a wavelength of 405 nm in an ELISA reader (Thermo Electron Corporation Multi Scan EX).

Forty healthy inbred Balb/c mice (*Mus musculus*) (6/8 weeks and – 25 g) were housed for at least 14 days in an environmentally-controlled room (temperature: 24 – 26°C ± 2°C, humidity: 55% ± 5%, 12-hour light/dark cycle) with access to food and water *ad libitum* and were used as the subjects for the present study. The guidelines followed were approved by the Animal Ethical and Welfare Committee, University of Kalyani (Vide: KU/IAEC/Z-11/07; dated: 18 May 2007). Thirty healthy mice were randomly selected for experimental purpose and were subdivided into five groups of six mice each. In Group 1, the negative control, six mice were fed a normal diet and given water *ad libitum*. This group served as the normal control. Group 2, the co-mutagenic control, was a subgroup of twenty-four mice that were force-fed with BaP at a dose of 25 mg/kg

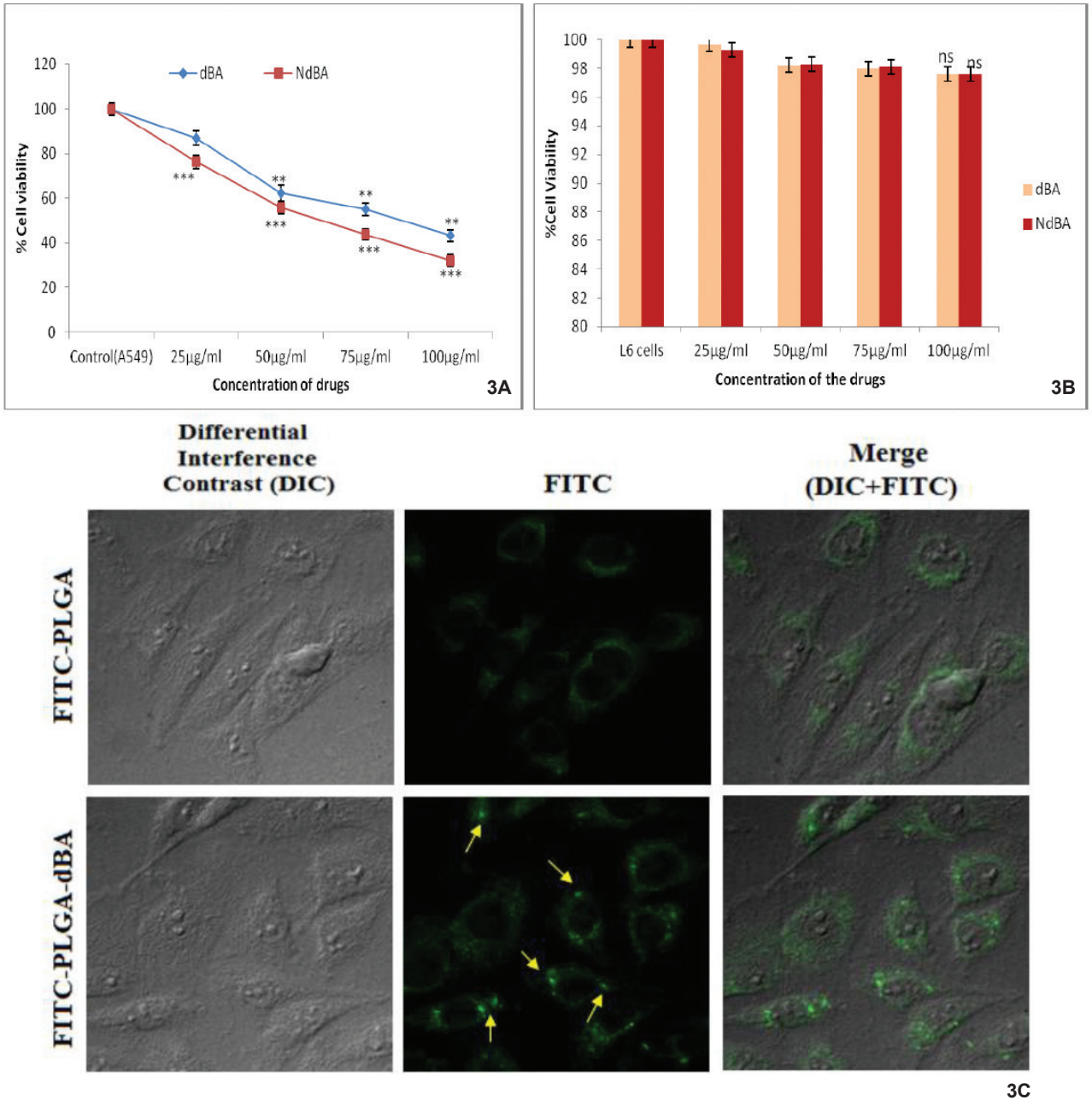

Figure 3 (A) Cellular cytotoxicity assay of A549 lung cancer cells, (B) cellular cytotoxicity assay of normal L6 skeletal muscle cells, and (C) confocal microscopic studies for cellular entry of nanoparticles in A549 cells.

dBA, derivative of betulinic acid; NdBA, nano derivative of betulinic acid; DIC, differential interference contrast, FITC, fluorescein isothiocyanate; PLGA, poly (lactide-co-glycolide).

body weight (b.w.) and SA at a dose of 10 mg/kg b.w. twice a week successively for 4 weeks to induce lung cancer at the 16th week [9]. Group 3, the drug-treated subgroup, was a subgroup of six mice taken from the co-mutagenic group (Group 2) that were force-fed with dBA at a dose of 20 mg/kg b.w. per day for 30 days. Groups 4 and 5, the nano drug-treated subgroups (dose 1 and dose 2, respectively), were two subgroups of 6 mice each (12 total) that were randomly selected from the co-mutagenic group of mice (Group 2) that were force-fed through gavage at a dose of 0.2 mg/kg b.w./day of NdBA (I) and at a dose of 0.3 mg/kg b.w./day of NdBA (II) for 30 days.

In a range finding trial, the doses of dBA, NdBA (I) and NdBA (II) were standardized by feeding 10 mg/kg b.w./day, 20 mg/kg b.w./day and 30 mg/kg b.w./day of dBA and 0.1 mg/kg b.w./day, 0.2 mg/kg b.w./day and 0.3 mg/

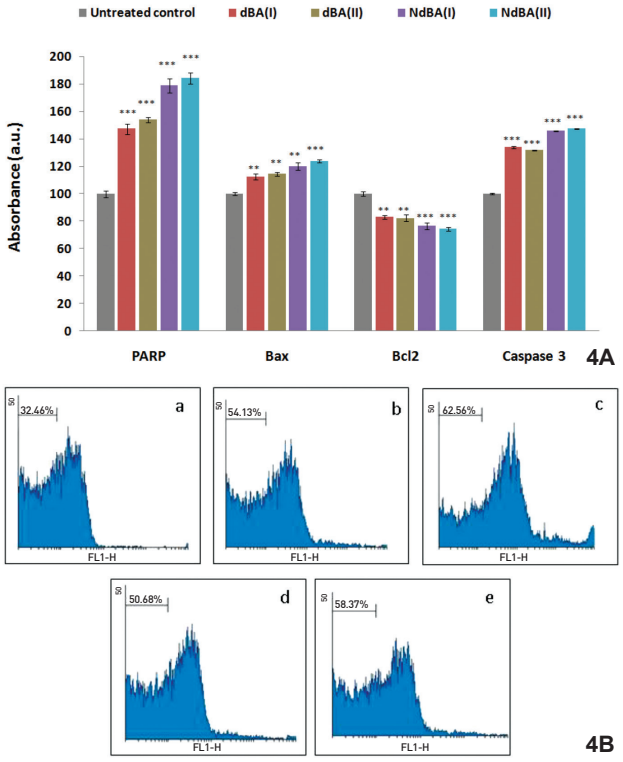

Figure 4 (A) Expressions of PARP, Bax and Bcl2 proteins according to indirect ELISA. (B) ROS generation studies of experimental sets of alveolar cells isolated from mice: a = normal control, b = co-mutagenic control, c = co-mutagenic + dBA, d = co-mutagenic + NdBA(I), and e = co-mutagenic + NdBA(II).

dBA, derivative of betulinic acid; NdBA, nano derivative of betulinic acid; PARP, poly (ADP-ribose) polymerase; Bax, Bcl2 Antagonist X; Bcl2, B-cell lymphoma 2; ELISA, enzyme-linked immunosorbent assay; ROS, reactive oxygen species.

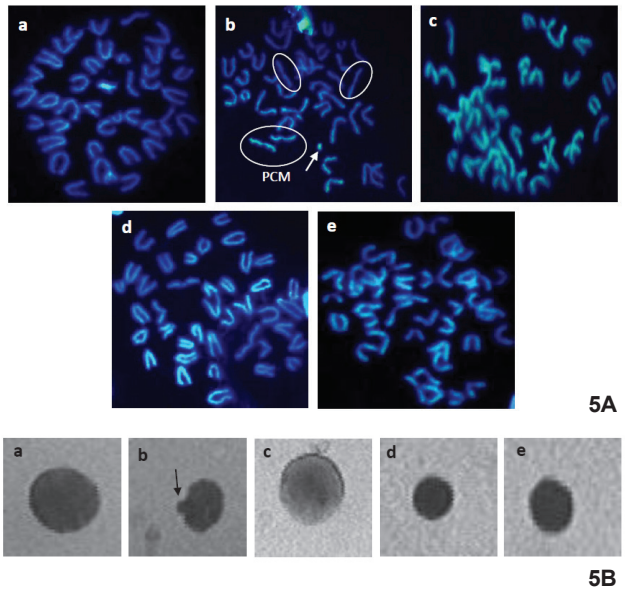

Figure 5 (A) Chromosomal study of metaphase complements and (B) bone marrow smears showing normal/micronucleated erythrocytes in different groups of mice: a = normal control, b = co-mutagenic control, c = co-mutagenic + dBA, = co-mutagenic + NdBA(I), and e = co-mutagenic + NdBA(II).

dBA, derivative of betulinic acid; NdBA, nano derivative of betulinic acid.

kg b.w./day of NdBA to the co-mutagenic control group of mice. For economy of cost and lives of the mice, trial doses of 20 mg/kg b.w./day for dBA and 0.2 mg/kg b.w./day and 0.3 mg/kg b.w. of NdBA were selected for further studies based on significant modulation in the nuclear condensation of perfused lung cells.

Lung tissues from the different groups of mice were removed aseptically and perfused in DMEM medium [5]. Nuclear condensation and DNA damage were quantified in isolated alveolar cells by using the cell-permeable fluorescent dye DAPI (4′,6-diamidino-2-phenylindole) [5] and were analyzed by using a fluorescence-activated cell-sorting (FACS, BD ARIA) analysis. In this study, widely-accepted and standard cytogenetical protocols were adopted for assessing chromosome aberrations (CAs) and micronuclei (MN) [5] to determine and analyze the changes in the chromosome morphologies in the different control and experimental sets of mice.

Lung tissues from control and experimental sets of mice were dissected, fixed in 10% normal buffered formalin for 24 hours, dehydrated in ascending concentrations of ethanol, cleared in xylene, and embedded in paraffin to prepare the block. For preparation and staining of the histological slides, the standard protocol for hematoxylin and eosin (H&E) staining was followed [7], and the slides were observed under a phase contrast microscope.

To specifically determine whether NdBA had the ability to cross the BBB, we orally fed NdBA to five mice at a dose 0.3 mg/kg b.w. twice per day for 7 days. At the end of the treatment period, mice were sacrificed *via* cervical dislocation. Brain tissues were prepared for TEM microscopy as per the standard procedure mentioned earlier [10].

Control A549 cells and both dBA- and NdBA-treated cells were isolated in PBS and washed once in cold PBS. Cells were fixed in 3% paraformaldehyde and suspended in 1 mL of propidium iodide (PI) solution containing 50 mg/mL of PI, 0.1% (w/v) sodium citrate, and 0.1% (v/v) Triton X-100. Cells were incubated at 4°C in the dark for 15 minutes and analyzed for possible cell-cycle arrest by using a flow cytometer (BD Calibur).

All data were obtained from three independent experiments. Statistical analyses were used to determine the level of significance based on differences between the mean values by using the student's *t*-test.

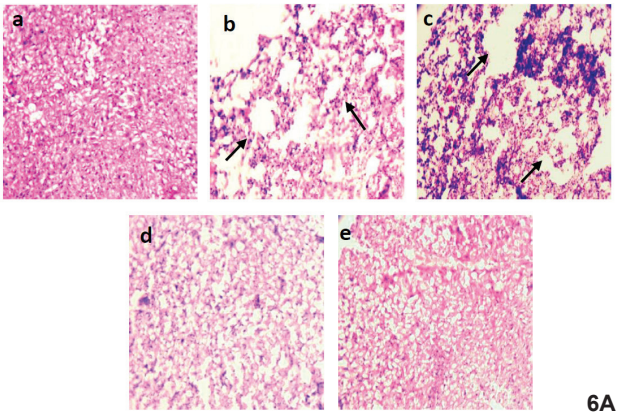

6A

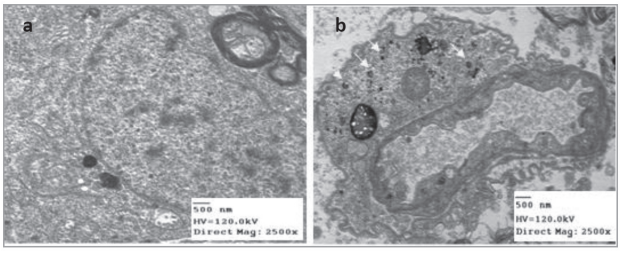

6B

Figure 6 (A) Histological analyses of lung tissues before and after treatment with co-mutagens and drugs: a = normal control, b = co-mutagenic control, c = co-mutagenic + dBA, d = co-mutagenic + NdBA(I), and e = co-mutagenic + NdBA(II). (B) Transmission electron microscopy images of brain tissue to detect the capability of NdBA to cross the blood brain barrier: a = normal mouse without any nanoparticle administration, b = mouse brain after administration of NdBA(II). The arrowheads mark the presence of NdBA, and Nu stands for nucleus.

dBA, derivative of betulinic acid; NdBA, nano derivative of betulinic acid.

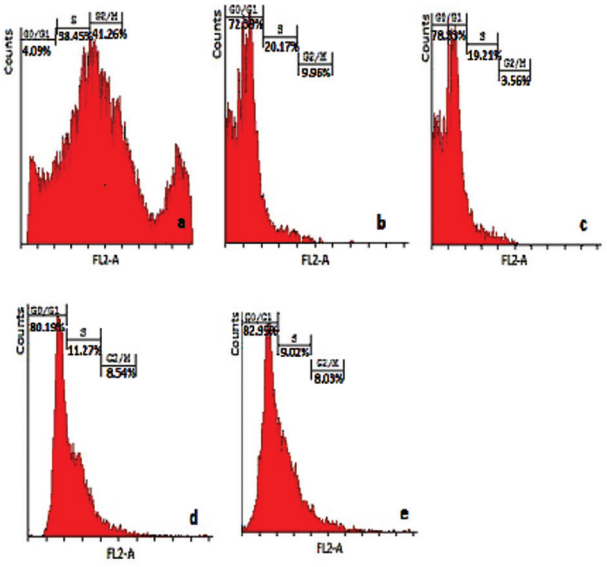

Figure 7 Nanopharmaceutical Approach for Enhanced Anti-cancer Activity of Betulinic Acid in Lung-cancer Treatment via Activation of PARP: Interaction with DNA as a Target.

Cell cycle analysis in A549 cells. a, Control A549 cells; b, dBA(I); c, dBA(II); d, NdBA(I); e, NdBA(II).
dBA, derivative of betulinic acid; NdBA, nano derivative of betulinic acid.

3. Results

NdBA had a smooth surface morphology without any pinholes or cracks. The mean diameter of NdBA was observed to be 110 ± 5 nm (Figs. 1A, 1B). An increase in the smearing of CT-DNA was observed on addition of dBA + CT-DNA and NdBA + CT-DNA, respectively; this would indicate an interaction of the drug and DNA had taken place and that the drugs had strong binding abilities with DNA as a target (Fig. 1C).

Analysis of the circular dichroism (CD) spectra of CT-DNA revealed a positive band at 275 nm and a negative band at 247 nm, which are characteristic features of right-handed B-form DNA. dBA and NdBA did not show CD spectra when they were free in the solution. Significant increases in the intensities of the positive and the negative bands were observed in the CT-DNA + dBA and CT-DNA + NdBA sets; the latter showed a greater increase, indicating that the binding and interaction of NdBA with CT-DNA were stronger than they were for dBA (Fig. 2A). Analysis of the Tm values of CT-DNA (82.5 ± 0.5°C), CT-DNA + dBA (85.0 ± 0.5°C) and CT-DNA + NdBA (92.5 ± 0.5°C) indicated that the increase in the Tm value on addition of NdBA was greater than it was for dBA (Fig. 2B).

A dose-dependent increase in cytotoxicity was observed in the dBA- and the NdBA-treated series of A549 cells after 24 hours of treatment. The IC_{50} value of both dBA and NdBA was found to be 50 μg/mL (Fig. 3A). Therefore, A549 cells were treated with two doses (50 μg/mL, IC_{50} dose, and 100 μg/mL, double the IC_{50} dose) of both dBA and NdBA for further studies. No significant changes in the cell viability percentages of L6 cells were observed among the drug-treated series, dBA-, NdBA (I)- and NdBA (II)-treated series, when compared to the untreated control (Fig. 3B).

Both FITC-PLGA particles (serving as FITC control) and FITC-PLGA-loaded dBA nanoparticles were taken up by the A549 cells after 3 hours of treatment, but both were confined to the cytoplasm; i.e., neither showed up inside the nucleus (Fig. 3C); this would indicate that the PLGA coat disintegrated in the cytoplasm, releasing the drug particles (dBA and NdBA) which then entered the nuclei of the A549 cells for more effective action.

Significant up-regulations in the expressions of PARP,

Bax and caspase 3 proteins and down-regulations in the expressions of the Bcl2 proteins were observed in dBA- and NdBA-treated A549 cells as compared to the untreated control cells, indicating that apoptosis had occurred in the cancer cells. NdBA (II) showed a relatively stronger apoptotic activity (Fig. 4A). Increases in the incidences of nuclear condensation and DNA damage with increasing dose of dBA and NdBA were revealed from the results of the FACS study. Cell pellets were observed under DAPI staining, and NdBA (II) was seen to have the greatest effect (Fig. 4B).

Various types of CAs of both minor and major types and MN were observed in the co-mutagenic treatment group. However, the incidences of both CAs and MN were found to be decreased in the dBA- and the NdBA-treated series. NdBA (II) showed better ameliorative potential (Figs. 5A, 5B).

Increases in the degradation and the loss of the architecture of pulmonary tissues were observed in the co-mutagenic group of mice when compared to the untreated control mice. However, after treatment with dBA and NdBA, visible improvements in the structural contour could be observed in the drug-treated cells. This improvement was particularly obvious in the NdBA-treated mice (Fig. 6A). After 10 days of NdBA treatment, the nanoparticles were found to be internalized in the brain tissue of the mice. Thus, NdBA could readily and effectively cross the BBB (Fig. 6B). As shown in Fig. 7, exposure of human A549 lung cancer cells to dBA and NdBA resulted in significant increases in the proportion of sub G0/G1 phase cells: 72.39% (dBA-I), 78.33% (dBA-II), 80.19% (NdBA-I) and 82.95% (NdBA-II).

4. Discussion

The results of the present study indicate that we successfully loaded dBA with PLGA nanoparticles for effective drug delivery. The nanoparticles were quite small, and they had spherical shapes with smooth surfaces and without any particle aggregation. Our findings further suggest that NdBA was stable and suitable for cellular entry. The negative zeta potential also helped the drugs to enter cells faster, making drug bioavailability more target specific. The results of CD spectroscopy and Tm profiles indicate that both dBA and NdBA had the ability to bind with CT-DNA and could cause changes in the conformation and the helicity of DNA (at 273 nm due to base stacking and at 245 nm the negative one was due to right-handed helicity), leading to an alteration of the DNA structure [11]. NdBA interacted with DNA more strongly than did dBA. Further, the thermal denaturation of CT-DNA with a subsequent rise in temperature was most likely due to the interaction and incorporation of dBA and NdBA into the CT-DNA. When the temperature of a DNA-containing solution increases, double stranded DNA is known to dissociate into single stranded DNA and produce a hyper chromic shift on the absorption spectra of DNA bases due to breaks in the covalent hydrogen bonds. The Tm, which is the temperature where half of the total number of base pairs remains unbonded, is usually introduced in order to identify this conversion process. Reports in the literature suggests [12] that intercalation of natural or synthesized organic and metallo-intercalators generally results in a considerable increase in melting temperature. In the present study also, Tm showed an increase by 10°C after incubation with NdBA.

Both dBA and NdBA had very negligible cytotoxic effects on normal L6 skeletal muscle cells, thus demonstrating their preferential sensitivity to cancer cells. Further, images of the intracellular uptakes of dBA and NdBA in A549 cells through confocal microscopic analysis confirmed that the cellular uptake of NdBA was faster than that of dBA. This finding would suggest that NdBA could increase the cellular uptake of a drug, thereby generating preferential and target-specific cytotoxicity in cancer cells.

Apoptosis is a vital mechanism that controls tissue kinetics by cell division and cell death [13]. Caspases are involved in apoptosis and act either as initiators or effectors. Caspase 3 is most important as it is involved in the final disassembly of the cell by cleaving a variety of cell structure proteins and generating DNA breaks [14]. This was confirmed in the present study. Major changes were observed in DNA laddering tests. CA and MN studies revealed a considerable increase in the MN and the CA frequencies in mice intoxicated with the co-mutagen; prevalence was lowered by the administration of dBA and NdBA, more by the administration of NdBA. Whenever a DNA strand breaks due to oxidative stress, PARP is activated. However, the cleavage of PARP by caspase 3 inactivates it and restrains PARP's DNA-repairing abilities. In order to examine the major apoptotic pathway involved, we studied the PARP activities. Indirect ELISA studies showed that the anti-apoptotic Bcl-2 expression level correlated with its intracellular ratio to Bax. p53 induces apoptosis by increasing the transcriptional activity of pro-apoptotic genes, such as Bax, or by repressing the activities of the anti-apoptotic genes of the Bcl-2 family.

The results of the FACS study revealed that both dBA and NdBA interfered with the proliferation of lung-cancer cells. The drugs arrested the A549 cells at the G0-G1 stage, indicating that the drugs interfered with the replication process and further confirming that the drug-DNA interaction could, indeed, cause conformational changes, possibly by cross-linking of the drugs with the DNA, which, in turn, could inhibit DNA replication.

Smaller sized nanoparticles in different nanometer ranges have been reported to facilitate the crossing of various biological barriers, such as the BBB and the tight junctions of various epithelial layers. Its small size and smooth surface gave NdBA faster mobility and the ability to cross the blood-brain barrier. The present findings imply that the PLGA-encapsulated derivative of betulinic acid (NdBA) had better efficacy than the un-encapsulated form of dBA against co-mutagenic (SA + BaP)-induced lung cancer in mice *in vivo* and A549 cells *in vitro*, making it a cost effective (at almost – 10 fold reduced dose than dBA) anti-cancer agent for use in therapeutic oncology.

Acknowledgment

This work was partially supported by a grant to Prof. A.

R. Khuda-Bukhsh, Department of Zoology, University of Kalyani, by Boiron Laboratories, Lyon, France. JD is grateful to DST-PURSE 2014-2015 for providing a Research Associate (RA) fellowship. ARK-B is grateful to University Grants Commission (UGC) for providing him an Emeritus Fellowship.

Conflict of interest

The authors declare that there are no conflict of interest.

References

1. Pershagen G, Nordberg G, Björklund NE. Carcinomas of the respiratory tract in hamsters given arsenic trioxide and/or benzo[a]pyrene by the pulmonary route. Environ Res. 1984;34(2):227-41.
2. Deng GE, Rausch SM, Jones LW, Gulati A, Kumar NB, Greenlee H, *et al*. Complementary therapies and integrative medicine in lung cancer: diagnosis and management of lung cancer, 3rd ed: american college of chest physicians evidence based clinical practice guidelines. Chest. 2013;DOI: 10.1378/chest.12-2364.
3. Ellingwood F. The American Materia Medica, Therapeutics and Pharmacognosy. Portland: Eclectic Medical Publications; 1919. 470 p.
4. Wang L, Bai L, Nagasawa T, Hasegawa T, Yang X, Sakai J, *et al*. Bioactive triterpene saponin from the roots of Phytolacca americana. J Nat Prod. 2008;71(1):35-40.
5. Das J, Das S, Samadder A, Bhadra K, Khuda-Bukhsh AR. Poly (lactide-co-glycolide) encapsulated extract of phytolacca decandra demonstrates better intervention against induced lung adenocarcinoma in mice and on A549 cells. Eur J Pharm Sci. 2012;47(2):313-24.
6. Fessi H, Puisieux F, Devissaquet JP, Ammoury N, Benita S. Nanocapsule formation by interfacial polymer deposition following solvent displacement. Int J Pharm. 1989;55(1):1-4.
7. Samadder A, Das J, Das S, De A, Saha SK, Bhattacharyya SS, *et al*. Poly(lactic-co-glycolic) acid loaded nano-insulin has greater potentials of combating arsenic induced hyperglycemia in mice: some novel findings. Toxicol Appl Pharmacol. 2013;267(1):57-73.
8. Das S, Das J, Samadder A, Paul A, Khuda-Bukhsha AR. Strategic formulation of apigenin-loaded PLGA nanoparticles for intracellular trafficking, DNA targeting and improved therapeutic effects in skin melanoma in vitro. Toxicol Lett. 2013;223(2):124-38.
9. Tran PH, Prakash AS, Barnard R, Chiswell B, Ng JC. Arsenic inhibits the repair of DNA damage induced by benzo(a)pyrene. Toxicol Lett. 2002;133(1):59-67.
10. Samadder A, Chakraborty D, De A, Bhattacharyya SS, Bhadra K, Khuda-Bukhsh AR. Possible signaling cascades involved in attenuation of alloxan-induced oxidative stress and hyperglycemia in mice by ethanolic extzxdzract of Syzygium jambolanum: drug-DNA interaction with calf thymus DNA as target. Eur J Pharm Sci. 2011;44(3):207-17.
11. Kong DM, Wang J, Zhu LN, Jin YW, Li XZ, Shen HX, *et al*. Oxidative DNA cleavage by schiff base tetraazamacrocyclic oxamido nickel(II) complexes. J Inorg Biochem. 2008;102(4):824-32.
12. Jain SS, Polak M, Hud NV. Controlling nucleic acid secondary structure by intercalation: effects of DNA strand length on coralyne-driven duplex disproportionation. Nucleic Acids Res. 2003;31(15):4608-15.
13. Hengartner MO. The biochemistry of apoptosis. Nature. 2000;407(6805):770-6.
14. Enari M, Sakahira H, Yokoyama H, Okawa K, Iwamatsu A, Nagata S. A caspase-activated DNase that degrades DNA during apoptosis, and its inhibitor ICAD. Nature. 1998;391(6662):43-50.